Journal of Applied Polymer Science

WILEY

Applied Polymer SCIENCE

RESEARCH ARTICLE OPEN ACCESS

Enhancing Flexibility and Adhesion of PVDF Coatings on PVC Textiles via PVDF/PMMA/Plasticizer Blends

Anya Sonnendecker | Johan Labuschagne

Department of Chemical Engineering, Faculty of Engineering, Built Environment & IT, University of Pretoria, Pretoria, South Africa

Correspondence: Anya Sonnendecker (u28097204@tuks.co.za)

Received: 7 January 2025 | **Revised:** 19 March 2025 | **Accepted:** 4 April 2025

Funding: The authors received no specific funding for this work.

Keywords: adhesion | flexible coatings | plasticizers | polymethyl methacrylate | polyvinylidene fluoride | PVC textiles | UV protection

ABSTRACT

This study investigated improving the flexibility and adhesion of polyvinylidene fluoride (PVDF) coatings on polyvinyl chloride (PVC) textiles by blending PVDF with polymethyl methacrylate (PMMA) and adding plasticizers. Because PVDF is inherently stiff, blends were prepared with 10 wt%, 30 wt%, and 50 wt% PMMA. Four plasticizers—di(propylene glycol) dibenzoate (P2), dibutyl phthalate (P3), di(ethylene glycol) dibenzoate (P4), and benzyl butyl phthalate (P5)—were also incorporated into 10 wt% PMMA blends. Thin films and coatings were produced via solution casting and dip-coating, then characterized using differential scanning calorimetry (DSC), dynamic mechanical thermal analysis (DMA), and scanning electron microscopy (SEM). A 10 wt% PMMA concentration improved adhesion and raised crystallinity (46.95% versus 30.87% for pure PVDF), while higher PMMA resulted in amorphous structures. Plasticizers lowered melting temperatures by up to 12°C and glass transition temperatures by up to 81.4°C (for P3), increasing flexibility. SEM revealed that plasticizers P3 and P4 generated uniform, nonporous morphologies, making them promising for UV-protective coatings. These blends maintained strong adhesion to PVC and demonstrated good mechanical performance. Further studies on UV stability are advised to confirm their long-term durability. DSC indicated increased thermal stability in PVDF/PMMA blends, while DMA confirmed enhanced mechanical integrity and material performance.

1 | Introduction

Polyvinylidene fluoride (PVDF) is a semicrystalline polymer valued for its outstanding weather resistance, chemical stability, and gloss retention, making it a popular choice for protective coatings across various industries [1, 2]. Pure PVDF-based coatings are typically applied to rigid structures [3, 4], like metal, due to the polymer's inherent stiffness, which limits its use on flexible substrates like architectural textiles such as PVC tarps [5]. Advancements in polymer chemistry have enabled the production of flexible PVDF copolymers [6, 7], expanding their use in flexible coating formulations. However, the production of these copolymers often requires sophisticated infrastructure, which may be lacking or too expensive for underdeveloped countries.

This research is part of a larger project focused on developing more affordable construction materials for housing in underdeveloped regions, with a primary emphasis on utilizing architectural textiles, particularly PVC-coated polyester tarps. However, non-UV-protected textiles have a very short lifespan; hence the need for the development of a less expensive, easy-to-produce flexible PVDF-based protective topcoat.

As an alternative to the creation of complex copolymers, the addition of plasticizers could be considered to enhance PVDF's flexibility. However, there is a significant scarcity of research available focused on identifying effective plasticizers specifically for the production of flexible coatings. Most research focuses on plasticizers, more often called diluents, used in the

melt processing of PVDF [8], in the creation of membranes for filtration [9], in the optimization of PVDF's piezoelectric properties [10–12], or their effects on the mechanical properties of hard elastic fibers [10].

A patent published by [13] provided some guidance in the field of selecting a suitable plasticizer. The patent suggested that adding small quantities of specific esters could enhance PVDF's flexibility. Yet, the effects of these esters on the morphology and physical properties of high molecular weight PVDF thin films remain unexplored.

In addition to PVDF's inherent rigidity concern, PVDF coatings often struggle with poor adhesion to most substrates due to PVDF's innate chemical inertness [3]. Generally, in the industry, an acrylic polymer, most prominently polymethyl methacrylate (PMMA), is added to aid with adhesion [4, 14, 15]. Several studies have been performed on the blending and miscibility of PMMA and PVDF [16–25]. These studies not only highlight the different applications for these blends but also the effect that the incorporation of different concentrations of PMMA has on several thermal, morphological, and mechanical properties of PVDF. However, most of the available literature focuses on the formation and controlled production of the piezoelectric β-crystal phase of PVDF by incorporating PMMA.

Typically, PVDF-based coatings contain 70 wt%–80 wt% PVDF, with the remainder being a compatible acrylic. Increasing the acrylic content beyond 30 wt% can significantly reduce PVDF's crystallinity, potentially diminishing mechanical reinforcement, weathering resistance, and chemical stability. Research indicates that PVDF-acrylic blends with more than 70 wt% PVDF maintain the dominant pure PVDF crystalline phase, which is crucial for preserving protective properties [5].

The primary aim of this research was to develop a flexible, adhesive PVDF-based protective coating suitable for use in architectural textiles, specifically PVC tarps, that would not require the use of sophisticated infrastructure to produce. To achieve this aim, the research focused on two key objectives. First, it examined the effect of varying PMMA concentrations in PVDF/PMMA-based thin films and coatings. Thin films were created through solution casting, while coatings were produced by dip-coating PVC tarps in a PVDF/PMMA-based solution. The study analyzed the thermal properties and surface morphology of the thin films, as well as the surface morphology of the coatings. Second, the research evaluated the flexibility of PVDF/PMMA-based thin films and coatings by assessing the impact of four different plasticizers—di(propylene glycol) dibenzoate, dibutyl phthalate, di(ethylene glycol) dibenzoate, and benzyl butyl phthalate. The plasticizers were selected from the list of esters proposed in the patent published by [13]. As a control, pure PVDF-based thin films and coatings were produced and analyzed in the same manner. The controls provided a baseline for considering the various factors that influence the surface morphology and crystal phase formation of PVDF during thin film formation, the most significant being the solvent evaporation rate [26]. This analysis aimed to identify the most effective combination to develop a protective topcoat that is flexible, adheres well to the PVC tarp, and possesses an optimal surface morphology for maximum UV protection.

2 | Experimental

2.1 | Raw Materials

Polyvinylidene fluoride (PVDF, Solef 6020/1001) powder was obtained from A. Schulman (currently part of LyondellBasell). Solef 6020/1001 possesses a melt flow index of 2 g / 10 min (measured at 230°C under a 21.6 kg load). Polymethyl methacrylate (PMMA, Altuglas V920T) pellets were purchased from Advanced Polymers PTY LTD; Altuglas V920T has a melt flow index of 6 g / 10 min (230°C, 3.8 kg load). N,N-Dimethylacetamide (DMAc, ReagentPlus, Sigma-Aldrich, Merch SA) was selected as the solvent for producing the thin films. The solvent was procured from Sigma-Aldrich (Merck SA) from their ReagentPlus range. All plasticizers used were procured from Sigma-Aldrich (Merck SA). All solvents and plasticizers were used as received without any extra purification.

To ease analysis and reporting, each plasticizer was designated a keyword as indicated below. Samples were named according to the weight percentage plasticizer and plasticizer key (e.g., PVDF/PMMA/P2 indicates that the sample contains PVDF, PMMA and plasticizer P2 (Di(propylene glycol) dibenzoate) in the sample) (Table 1).

2.2 | Method

2.2.1 | Operating Conditions Determination

Initial exploratory experiments were performed in house to determine the most important operating conditions, namely the solvent, solids concentration in solution, dissolution temperature, and drying temperature. These were all dependent on the specifications of the larger overarching project. The main aim of the overarching project was to produce a PVDF-based solution to be used as a UV-protective topcoat on PVC-coated polyester textiles applied via the dip-coating method. While the coating method dictated the solids concentration in solution due to the need for a particular viscosity, the degradation temperature of the base textile controlled the maximum drying temperature of the solution to create the thin film. The aim was to mimic the topcoat creation process as closely as possible.

Thermal gravimetric analysis (TGA) was used to determine the degradation temperature of the PVC-coated polyester textile. The results indicated that an absolute maximum drying temperature of 120°C could be used; however, for safety, a drying temperature of 100°C was selected.

TABLE 1 | Keywords awarded to each plasticizer to ease reporting.

Key	Chemical	Key	Chemical
P2	Di(propylene glycol) dibenzoate	**P4**	Di(ethylene glycol) dibenzoate
P3	Dibutyl phthalate	**P5**	Benzyl butyl phthalate

Next, the recommended solvent and solids concentration was determined. Our study considered the dissolution and stability of PVDF at room temperature and evaluated the performance of the four most well-known PVDF solvents—Dimethylacetamide (DMAc), Dimethylformamide (DMF), N-Methyl-2-pyrrolidone (NMP), and Dimethyl sulfoxide (DMSO)—across various PVDF concentrations (5 wt%, 10 wt%, 15 wt%, 20 wt%, 25 wt%, and 30 wt%).

It was concluded that the absolute maximum weight percentage of solids in solution was 20 wt% with most of the solvents, as any higher concentration caused the formation of very viscous or gel-like solutions. The results also showed, as can be seen in Figure 1, that DMAc was the only solvent that produced the clearest solution over the widest range of concentrations. The discoloration of the final solution was not just affected by solid concentration but also by dissolution temperature. As shown in Figure 2, the DMAc solution did not discolor with an increase in dissolution temperature. A dissolution temperature of 50°C was selected to make the system more energy-efficient and to minimize solvent evaporation during dissolution.

2.2.2 | Casting Solution Creation

2.2.2.1 | PVDF and PMMA-Blended Casting Solution. PVDF powder was dissolved in a beaker using DMAc as the solvent. The dissolution temperature was kept constant

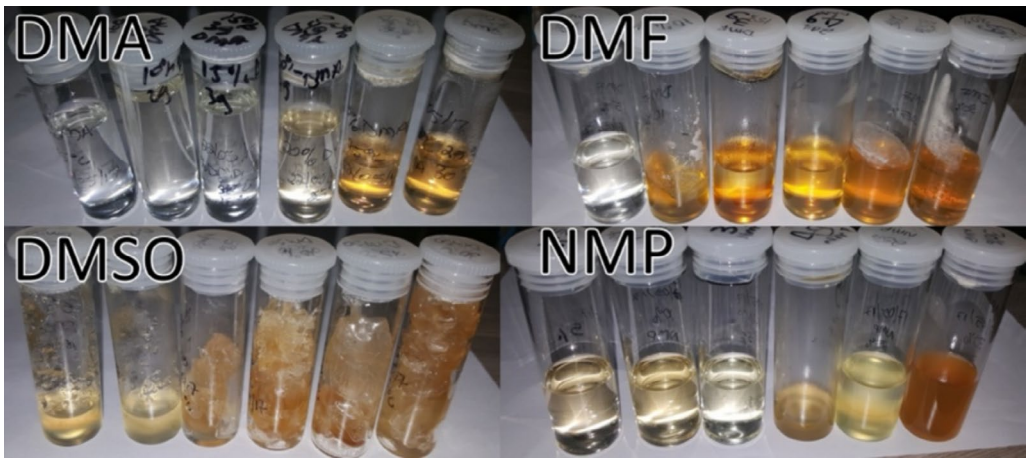

FIGURE 1 | Samples of the PVDF solution for each solvent taken at 25°C. For each solvent, the PVDF concentration increases from left to right, starting with a 5 wt% PVDF solution on the left and ending with a 30 wt% PVDF solution on the right, in increments of 5 wt% PVDF. [Color figure can be viewed at wileyonlinelibrary.com]

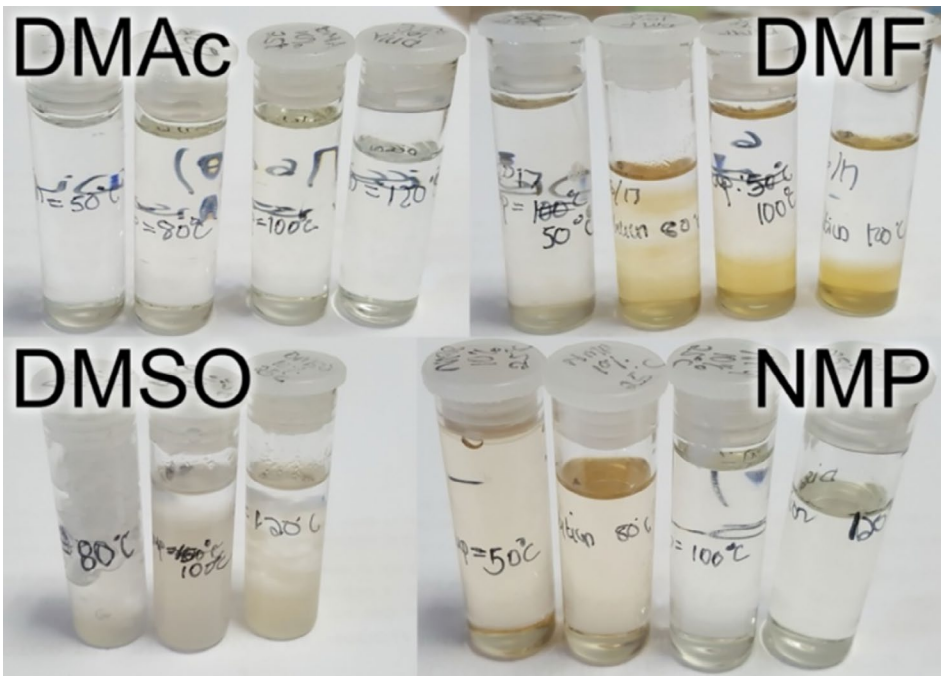

FIGURE 2 | Samples of PVDF solution for each solvent taken at 25°C. For each solvent, the dissolution temperature increased from left to right, starting at 50°C, 80°C, 100°C, and 120°C. Except for the DMSO solvent, as PVDF did not dissolve at 50°C. [Color figure can be viewed at wileyonlinelibrary.com]

at 50°C by submerging the beaker in a silicon oil bath. The solution was stirred continuously using a mechanical stirrer. After the dissolution of PVDF (approximately an hour dissolution time) a specified amount of PMMA granules was added and stirred for one hour. During this time, the stirrer rate was increased slightly, and the solution was left for one hour to ensure homogeneity.

Three different concentrations of PMMA were investigated: 10 wt% (PVDF/PMMA/10), 30 wt% (PVDF/PMMA/30) and 50 wt% (PVDF/PMMA/50). Enough solvent was used to ensure an 80:20 weight percentage ratio between the solvent and solids (PVDF and PMMA). Hence, in a sample denoted as PVDF/PMMA/30, 30 wt% PMMA and 70 wt% PVDF were used, which form part of the 20 wt% *solids* in the sample that was dissolved with 80 wt% DMAc.

2.2.2.2 | PVDF, PMMA and Plasticizer Blended Casting Solution. The same initial steps (dissolution of PVDF and PMMA) were performed to create the plasticized films. After the dissolution of PMMA, an equal amount of plasticizer (weight-based with regard to PVDF) was added. The stirring rate was increased slightly, and the solution was left for an hour to ensure homogeneity. Enough solvent was used to ensure an 80:20 weight percentage ratio between the solvent and solids (PVDF, PMMA and plasticizer). Hence, in a sample denoted as PVDF/PMMA/P2, 45 wt% PVDF, 45 wt% plasticizer P2, and 10 wt% PMMA were used, which forms part of the 20 wt% *solids* in the sample that was dissolved with 80 wt% DMAc.

2.2.3 | Thin Film and Coated Sample Creation

All castings and coatings were performed at 25°C. Hence, the casting solution was removed from the oil bath and left to cool to the desired temperature. Thin films were created by casting the solution on a clean glass surface, whereas the coatings were created by casting the solution on a 10 cm by 10 cm piece of PVC tarp. The solution was spread evenly over the relevant surface before drying at 100°C in a conventional convection oven for an hour. The samples were removed from the oven and left to cool to room temperature. The thin films were removed from the glass substrate by submerging them in warm water. The same method was used to produce a pure PVDF thin film and coated sample as a reference. A pure PVDF thin film and coated sample were created using the same method. The pure PVDF thin film is denoted as PVDFFilm, and the coating is PVDFCoating.

2.2.4 | Influencing Variable Considerations

To eliminate the effects of random variables that could influence the results, all processing parameters were kept strictly constant, including dissolution time and temperature, casting temperature, casting substrate, and drying temperature and duration. A drying temperature of 100°C—higher than the dissolution temperature of 50°C—was selected to negate any effects that the thermal history of the samples might have on the outcomes.

2.3 | Analytical Instruments

2.3.1 | FTIR: Spectral Analysis Method

FTIR spectra were generated using PerkinElmer Spectrum Timebase software on a PerkinElmer Spectrum 100 with an installed Universal ATR sampling Accessory. The instrument resolution was set at 4 cm^{-1} with a data interval of 1 cm^{-1}. The wavenumber range studied was 4000 cm^{-1} to 550 cm^{-1}. The force gauge on the ATR accessory was kept at 100 for all the samples while performing 32 scans per sample to ensure accuracy.

The generated spectra were smoothed, and the baseline was corrected utilizing the asymmetric least squares method proposed by [27]. Reference spectra for all raw materials were collected in house.

2.3.2 | DSC Analysis: PVDF Degree of Crystallinity, Melting and Crystallization Temperature Determination

A PerkinElmer DSC 4000 was used in combination with Pyris software for data analysis. Thermal curves were obtained in a N_2 atmosphere by heating the sample from 30°C to 250°C at a rate of 10°C/min, while crystallization curves were obtained by cooling the sample at the same rate from 250°C back down to 30°C.

The degree of crystallinity (X_C) of the thin films was determined using Equation (1) as given in [28] which is the same as the equation used in [29, 30].

$$X_c = \frac{\Delta H_m / \varphi}{\Delta H_o} \times 100 \quad (1)$$

where φ is the weight fraction PVDF in the blend, ΔH_m is the melting enthalpy measured, and ΔH_o is the melting enthalpy of PVDF at 100% crystallinity. The value of ΔH_o is 104.5 kJ/kg [31].

The cooling rate was shown to have a significant effect on the crystallization temperature in the nonisothermal cooling of PVDF/PMMA polymer blends [20]. Hence, the same cooling rate was used to analyze all samples to ensure fair sample comparability.

2.3.3 | Dynamic Mechanical Thermal Analysis (DMTA): Determination of the Glass Transition Temperature and Tarp Flexibility

The glass transition temperature (T_g) of the thin film samples was determined using a PerkinElmer DMA8000 dynamic mechanical analyzer. Samples were placed in PerkinElmer material pockets and subjected to single-cantilever mode with multifrequency oscillations at 1 Hz and 10 Hz. A displacement amplitude of 0.05 mm was applied over a temperature range from −100°C to 120°C, utilizing liquid nitrogen cooling to achieve the desired temperature range. The T_g was calculated as the average value obtained from three replicate measurements.

The flexibility of the dip-coated PVC tarps was analyzed using an isothermal time scan on the DMA8000. Samples were placed in material pockets and subjected to single-cantilever mode with multifrequency oscillations at 1 Hz and 10 Hz, with a displacement amplitude of 0.05 mm, at a constant temperature of 30°C. Each sample was held at this temperature for 60 min. The storage modulus was recorded for each sample to investigate the effect of the coatings on tarp flexibility.

2.3.4 | SEM Analysis: Thin Film Surface Morphology

The surface morphology of the thin films and coatings was examined using one of two instruments depending on availability: the Zeiss Crossbeam 540 FEG SEM or the Zeiss Ultra PLUS FEG SEM. All the samples were prepared for analysis by coating the surface with a thin layer of carbon in a Quorum Q150T Plus coating unit.

3 | Results and Discussion

3.1 | Pure PVDF Coating Analysis

The surface morphology (at the air–surface interface and the substrate–coating interface) of pure PVDF thin films was analyzed for samples cast on both glass and PVC-based tarp. The results, shown in Figure 3, highlight the distinct differences in surface texture depending on the substrate and interface. When coated on glass, PVDF coatings exhibited a notably smooth air–surface interface, whereas the PVC-coated samples displayed increased roughness.

Both coatings showed a certain amount of spherulite formation on the substrate–coating interface. On the glass, the PVDF coating exhibited sporadic spherulite formations surrounded by smoother amorphous regions. In contrast, the PVC tarp coatings formed a significantly rougher and porous surface with smaller, well-defined spherulites. These findings clearly show that the substrate properties strongly influence the coating morphology at both the air–surface and substrate–coating interfaces.

Similar results have been reported in the literature. Research conducted by [32] demonstrated comparable effects, where variations in the substrate led to corresponding changes in the formation and distribution of spherulite size. The research cited herein [33] studied this phenomenon further and demonstrated that there is an interplay between the polymer–substrate and solvent–substrate interactions. When the interaction between the polymer and substrate is stronger than that between the solvent and substrate, the polymer chains will preferentially wet the substrate, leading to a smoother, more uniform thin film.

Glass, being hydrophilic [3] with high surface energy, interacts differently with PVDF than the hydrophobic, low surface energy PVC tarp. As a hydrophobic polymer, PVDF aligns more favorably with the PVC tarp, where stronger van der Waals interactions promote attraction. Hence, the polymer–substrate attraction is stronger between PVDF and the PVC tarp than glass. Additionally, DMAc, a polar aprotic solvent, has a stronger interaction with glass caused by hydrogen bonds between the carbonyl oxygen of the solvent and the -OH groups of glass. Therefore, when coating on glass, the solvent–substrate interaction will dominate, causing dewetting of the polymer chains on the substrate surface. The opposite is true when coating occurs on the PVC tarp.

However, these interactions are not the sole factor influencing the morphology, specifically when it comes to the formation of PVDF spherulites. Research has shown that the rate at which a solvent evaporates significantly influences the morphology of the resulting film [26, 34–38]. Faster evaporation leads to the formation of smaller spherulites, often accompanied by pore development. In contrast, slower evaporation promotes the growth of larger, more uniform spherulites. In the case where the solvent preferentially wets the glass surface, a slight solvent concentration differential can occur between the air–surface and the substrate–surface interfaces. At the air–surface interface, solvent evaporation is accelerated due to the lower concentration, leading to the formation of smaller spherulites (Figure 3e). At the substrate–coating interface, solvent evaporation is slowed and the opposite occurs. On the other hand, when the polymer preferentially wets the surface of the tarp, the opposite effect occurs, causing a much higher solvent evaporation rate at the substrate–coating interface.

The thermodynamic properties of the substrate, particularly its heat transfer characteristics, also play a role in shaping these differences. The rough, heterogeneous surface of the PVC tarp increases nucleation site density for PVDF crystallization, facilitating the formation of smaller, densely packed spherulites. These conditions promote rapid crystal growth, which can trap residual solvent during the drying process, contributing to the observed porosity in the film (Figure 3f).

These results clearly demonstrate that the interaction between the substrate and the constituents of the coating should be considered when evaluating surface morphology and using this evaluation to select the optimal protective coating.

3.2 | PVDF/PMMA Blend Film and Coating Analysis

3.2.1 | DSC Analysis

The thermal properties of PVDF/PMMA blended thin films were analyzed for samples cast on glass. The DSC thermogram results presented in Figure 4 and Figure 5 confirm that the addition of PMMA reduced both the melting and crystallization temperatures of all the films. A direct correlation was observed between the increase in PMMA concentration and the decrease in both temperatures, except for the crystallization temperature of the PVDF/PMMA/50 sample, which was nonexistent due to the sample being fully amorphous.

The miscibility between PVDF and PMMA was established as none of the thermograms showed signs of peak separation.

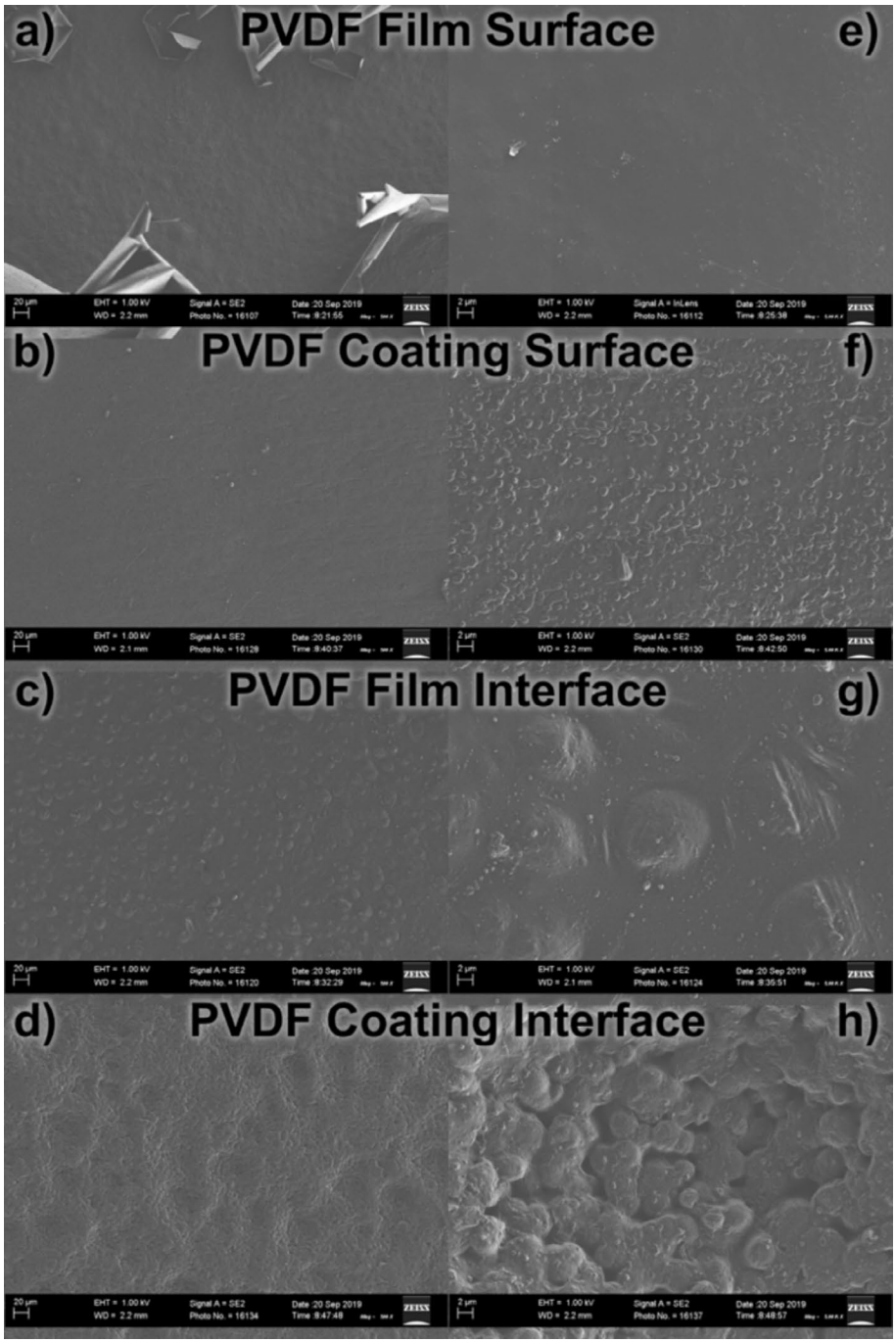

FIGURE 3 | Comparison of PVDF morphology on glass ("films") and plasticized PVC tarp ("coatings"). Images (a–d) show 500x magnification with a 20 μm scale bar, and (e–h) show 5000x magnification with a 2 μm scale bar. (a, e) depict air–surface morphology on glass; (c, g) show the glass substrate–coating interface. (b, f) present air–surface morphology on PVC tarp; (d, h) display the PVC substrate–coating interface.

The degree of crystallinity of the three different PMMA blended samples is displayed in Table 2. Interestingly, the degree of crystallinity increased for the thin film containing 10 wt% PMMA, which contradicts the results found in the majority of the literature [14, 19, 20, 39]. Based on the literature, the melting temperature, crystallization temperature, and degree of crystallinity are expected to decrease with an increase in PMMA concentration. However, in this case, PMMA may be acting as a nucleating agent, which could explain the rise in crystallinity (Table 2).

The increase in the degree of crystallinity at low PMMA concentrations could be explained by the two-step diffusion mechanism proposed by [22]. As described by [22], during the mutual diffusion process, PMMA molecules migrate away from areas of PVDF crystal formation; hence, they do not interfere with crystal growth. They can act as crystal nucleating sites, promoting the growth of more crystalline regions [30].

In the self-diffusion mechanism, the limited presence of PMMA reduces chain entanglement within the PVDF matrix,

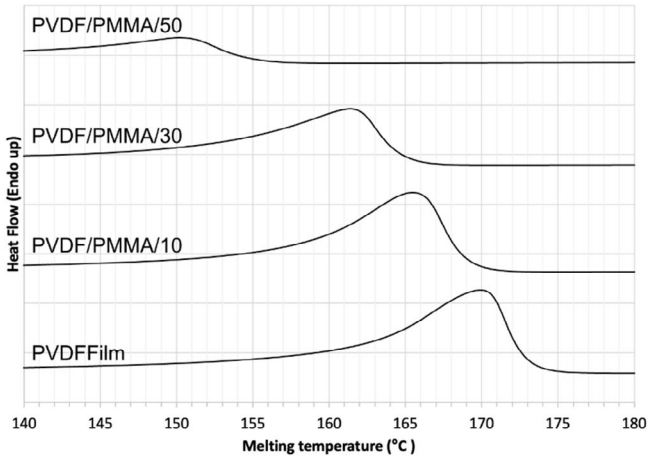

FIGURE 4 | PVDF/PMMA-blended thin film melting DSC thermograms compared to that of the pure PVDF thin film.

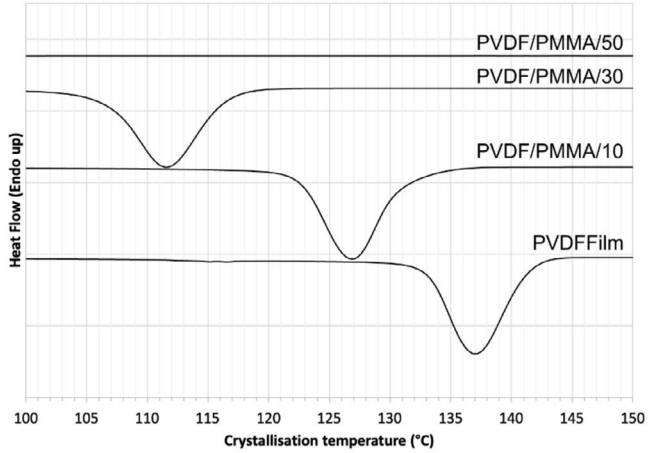

FIGURE 5 | PVDF/PMMA-blended thin films' crystallization DSC thermograms compared to that of the pure PVDF thin film.

TABLE 2 | The percentage crystallinity for all of the PMMA-containing PVDF-based thin films in comparison to the pure PVDF reference film.

Sample	Crystallinity (%)
PVDFFilm	30.87
PVDF/PMMA/10	46.95
PVDF/PMMA/30	39.28
PVDF/PMMA/50	30.57

allowing PVDF chains to move, align, and integrate into the crystalline structure more effectively. Although PMMA slightly slows the crystallization rate, this delay provides PVDF chains with more time to organize into well-defined crystalline regions. The combination of additional nucleation sites and a slower crystallization process results in an increased degree of crystallinity. This is reflected in the rise in the heat of crystallization from 43.5 J g^{-1} for pure PVDF to 57.47 J g^{-1} in the PVDF/PMMA/10 sample.

Even though PMMA may increase the degree of crystallinity, its presence impacts the perfection and stability of the crystals, reducing the melting temperature and delaying the onset of crystallization. The broadening of the melting curves with increasing PMMA concentration is due to the formation of a diverse range of crystals with varying degrees of perfection and stability.

PMMA concentrations exceeding 30 wt% to 40 wt% are associated with the formation of an amorphous structure, as demonstrated in multiple studies [18, 29, 40, 41]. The transition from a semicrystalline to an amorphous structure is heavily influenced by processing conditions, which likely explains the variability in reported results across the literature. In this investigation, the PVDF/PMMA/50 sample exhibited a fully amorphous structure, confirmed by the absence of any measurable heat of crystallization.

3.2.2 | SEM Analysis

The surface morphology of the different PVDF/PMMA blends coated on two different substrates (glass and PVC tarp) was analyzed and compared in Figure 6. The air–surface interface of the samples coated on glass all look similar, with no spherulites visible. The most significant morphology difference is observed in the sample of PVDF/PMMA/10 that was dip-coated onto the PVC tarp (Figure 6d). The surface appears to be rougher than that of the glass cast films and the other samples coated on the PVC tarp. This is likely due to two factors: the surface enrichment phenomena [3, 42] and the polymer–substrate versus solvent–substrate interaction [33], both of which are caused by the substrate properties. On the glass, PMMA preferentially enriches the substrate interface, leaving an enriched PVDF air–surface interface.

The rougher air–surface interface observed in the PVDF/PMMA/10 sample likely results from the interplay between the heterogeneous PVC tarp substrate and the low concentration of PMMA. This combination increases nucleation site density, leading to enhanced PVDF spherulite formation both at the interface and throughout the bulk of the coating. Consequently, this heightened nucleation activity influences the overall surface morphology. As the PMMA concentration increases, the nucleation effects decrease, and an increase in spherulite growth suppression occurs, resulting in a more even distribution of much smaller crystals and higher amorphous content (Figure 6 (e and f)).

Studies have shown that PMMA is miscible with PVC [43–47], a property attributed to specific interactions between the carbonyl groups of PMMA and the hydrogen atoms in the CH–Cl groups of PVC. In contrast, PVDF is not miscible with PVC [48]. However, the hydrophobic and Van der Waals forces interaction between PVDF and PVC does contribute to the polymer chain wetting of the tarp surface. Even though the interactions between PMMA and PVC are not stronger than those of PVDF, PMMA does improve the adhesion and compatibility of the coating to the tarp surface. This may be due to the favorable interaction between PMMA and the additives/plasticizers in the PVC tarp, enhancing the compatibility of the coating and the

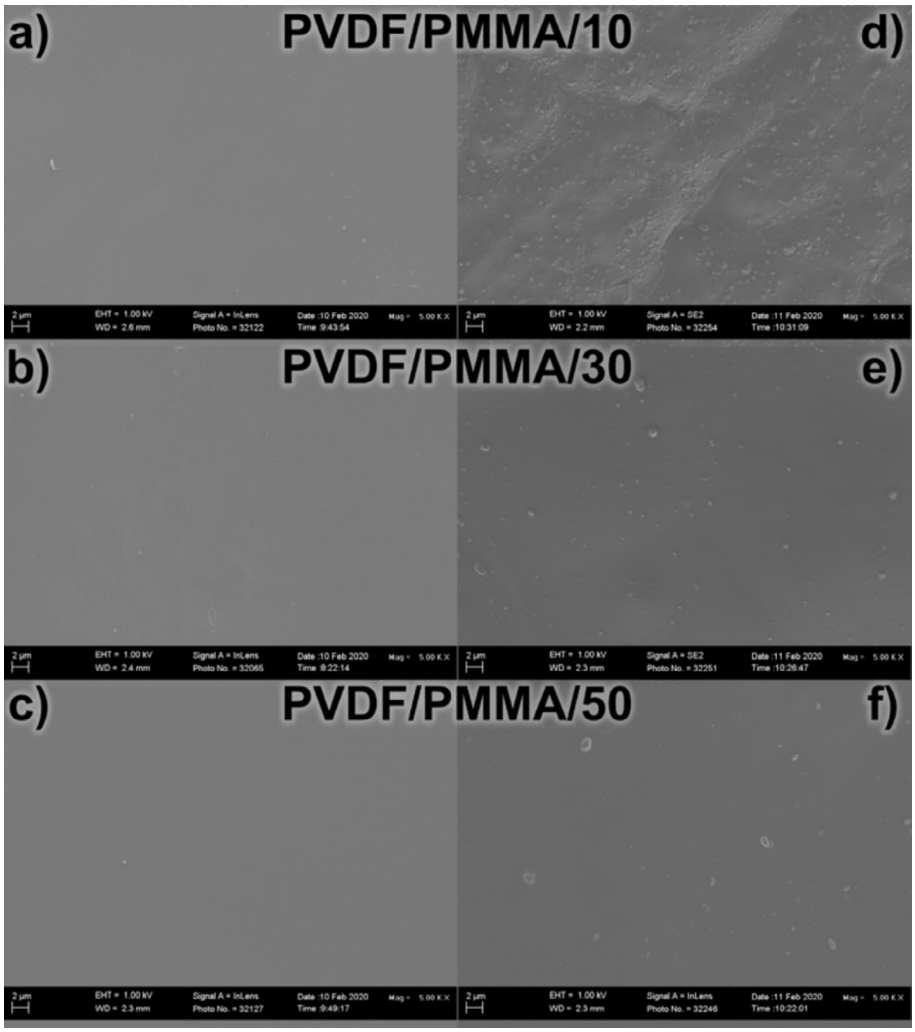

FIGURE 6 | SEM images of surface morphology for PVDF/PMMA-blended films (cast on glass) with 10 wt% (a), 30 wt% (b), and 50 wt% PMMA (c). Comparative images of the same compositions dip-coated onto a PVC tarp are shown in (d–f). The images are at 5000× magnification with a 2-μm scale bar.

surface. The increased adhesion is evidenced by the observation that none of the PMMA-containing coated samples exhibited any signs of delamination, whereas the sample coated with pure PVDF delaminated completely.

In summary, the results show that even a concentration as low as 10 wt% of PMMA can be used to improve the adhesion of PVDF to the PVC tarp and that all of the PMMA blended solutions produced coatings on the tarp that displayed a uniform surface morphology without any porosity or voids. Therefore, any of the blends could serve as the base coating solution for the next phase of the study, which involves analyzing and identifying the most suitable plasticizer. However, PVDF-based acrylic coating blends typically contain at least 70 wt% PVDF in the resin mixture [5]. Based on this, the decision was made to investigate the plasticization of films containing 10 wt% PMMA exclusively to balance the enhanced adhesion with the potential negative effects that the addition of acrylic might have on the mechanical and weathering properties of the PVDF-based coating [3].

3.3 | Plasticized PVDF/PMMA Film and Coating Analysis

3.3.1 | Plasticized Film Analysis

3.3.1.1 | DSC and SEM Analysis. The thermal properties of plasticized PVDF/PMMA thin films were analyzed to assess the effect of the plasticizer on the film's properties and to determine whether the mixture remains miscible across a wide range of operating conditions. This analysis aims to support the selection of the most suitable coating mixture.

All the produced films exhibited a single melting (Figure 7) and crystallization peak (Figure 8), confirming that all of the blends are miscible at these temperatures. The incorporation of plasticizers decreased the melting and crystallization temperatures of the PVDF/PMMA films. Plasticizers P3, P4, and P5 had the largest impact on the melting temperature—decreasing it by approximately 12°C.

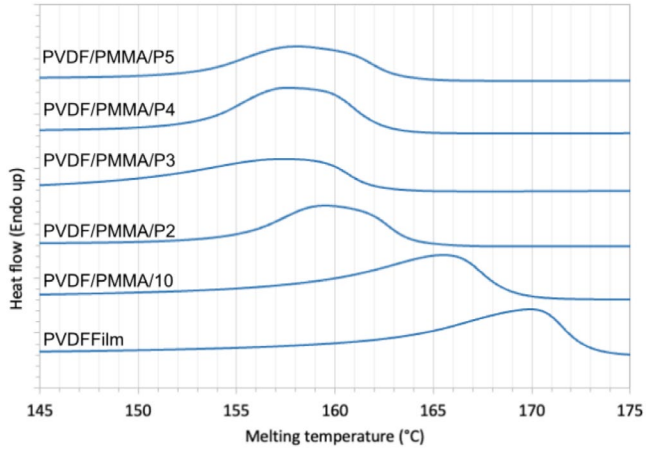

FIGURE 7 | Plasticized PVDF/PMMA films' melting DSC thermograms compared with a pure PVDF film and the PVDF/PMMA/10 film made under the same conditions. [Color figure can be viewed at wileyonlinelibrary.com]

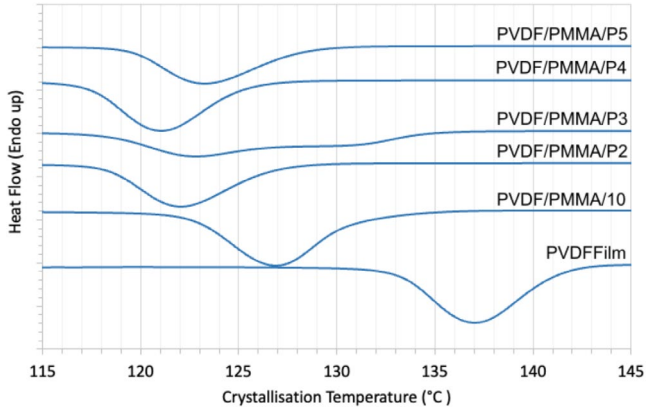

FIGURE 8 | Plasticized PVDF/PMMA film crystallization DSC thermograms compared with a pure PVDF film and the PVDF/PMMA/10 film made under the same conditions. [Color figure can be viewed at wileyonlinelibrary.com]

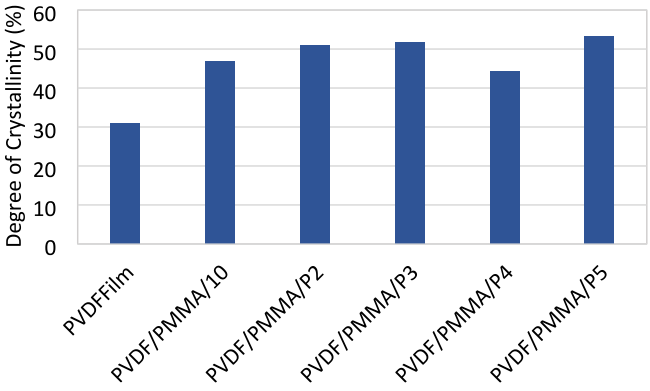

FIGURE 9 | Comparison of the degree of crystallinity determined by DSC for reference samples (PVDFFilm and PVDF/PMMA/10) and the PVDF/PMMA/plasticizer blends. [Color figure can be viewed at wileyonlinelibrary.com]

The plasticized films exhibited a broadening of their melting curves, indicating that the addition of plasticizers altered the crystallization behavior and thermal transition of PVDF within the PVDF/PMMA blend. DSC analysis showed that the degree of crystallinity of all the plasticized samples increased in comparison to the pure PVDF sample (Figure 9). Hence, the broadened melting curves suggest a reduction in crystal perfection, a greater variation in crystal sizes, or a combination of both effects. Examination of the surface morphology of the plasticized samples (Figure 10 (e,g, and h)) showed the formation of very large spherulites with a wide distribution in crystal sizes, supporting that both factors are contributing to the widening of the melting curve. In the case of sample PVDF/PMMA/P4, it seems that the crystal perfection plays a larger role in broadening the melting curve as the variation of spherulite sizes is less pronounced.

A significant broadening of the crystallization curve was observed in the PVDF/PMMA/P3 sample. The addition of P3 altered the crystallization kinetics, causing crystal formation to start at a higher temperature but also to extend over a larger range than compared to the other plasticizers. This indicates that P3 increases the PVDF chain mobility, enabling it to start ordering into crystals at a higher temperature than compared to the PVDF/PMMA/10 sample. The crystallization peak height of PVDF/PMMA/P3 decreased significantly again, pointing to the heterogeneous nature of the crystalline domains.

The DSC peak shifts are also influenced by the intermolecular interactions between PVDF, PMMA, and each plasticizer. PMMA and PVDF exhibit dipole–dipole attractions between their carbonyl and CH_2-CH_2 groups, respectively. The addition of a plasticizer disrupts this interaction by competing for these dipole–dipole interactions, resulting in a shift in the thermogram peaks. Plasticizers P2 and P4 caused the most significant downshift in crystallization temperature. This may be due to their ether and ester groups that can interact with PMMA's carbonyl groups, which affects crystallization kinetics. Bulkier plasticizers like P3 and P5 introduce larger side groups that interfere with the regular packing of PVDF chains. This leads to the formation of less perfect crystals, resulting in a broader melting peak, especially in the case of P3. The very broad crystallization peak of PVDF/PMMA/P3 could also be attributed to the steric hindrance that P3 introduces due to its bulky nature. It is important to note that the exact mechanism of plasticization remains poorly understood, particularly in high-molecular-weight semicrystalline polymers, such as PVDF, which can coexist in multiple crystal conformations. Several theories have been proposed to explain the mechanism of plasticization, notably the gel theory, the lubrication theory, and the free volume theory [49].

The addition of plasticizers led to an increase in the degree of crystallinity, as shown in Figure 9. This suggests that the plasticizers either enhanced nucleation site density or effectively mobilized the PVDF polymer chains, enabling them to align more efficiently into crystalline structures. Examination of the surface morphology (Figure 10) reveals that, in the presence of both PMMA and plasticizers, the samples containing P2, P3, and P5 exhibited increased chain mobility due to the presence of very large spherulites. These plasticizers acted primarily as diluents concerning nucleation, resulting in the formation of larger, well-defined spherulites. In contrast, the addition of P4 predominantly increased nucleation sites, leading to the development of smaller, more evenly distributed spherulites. It should

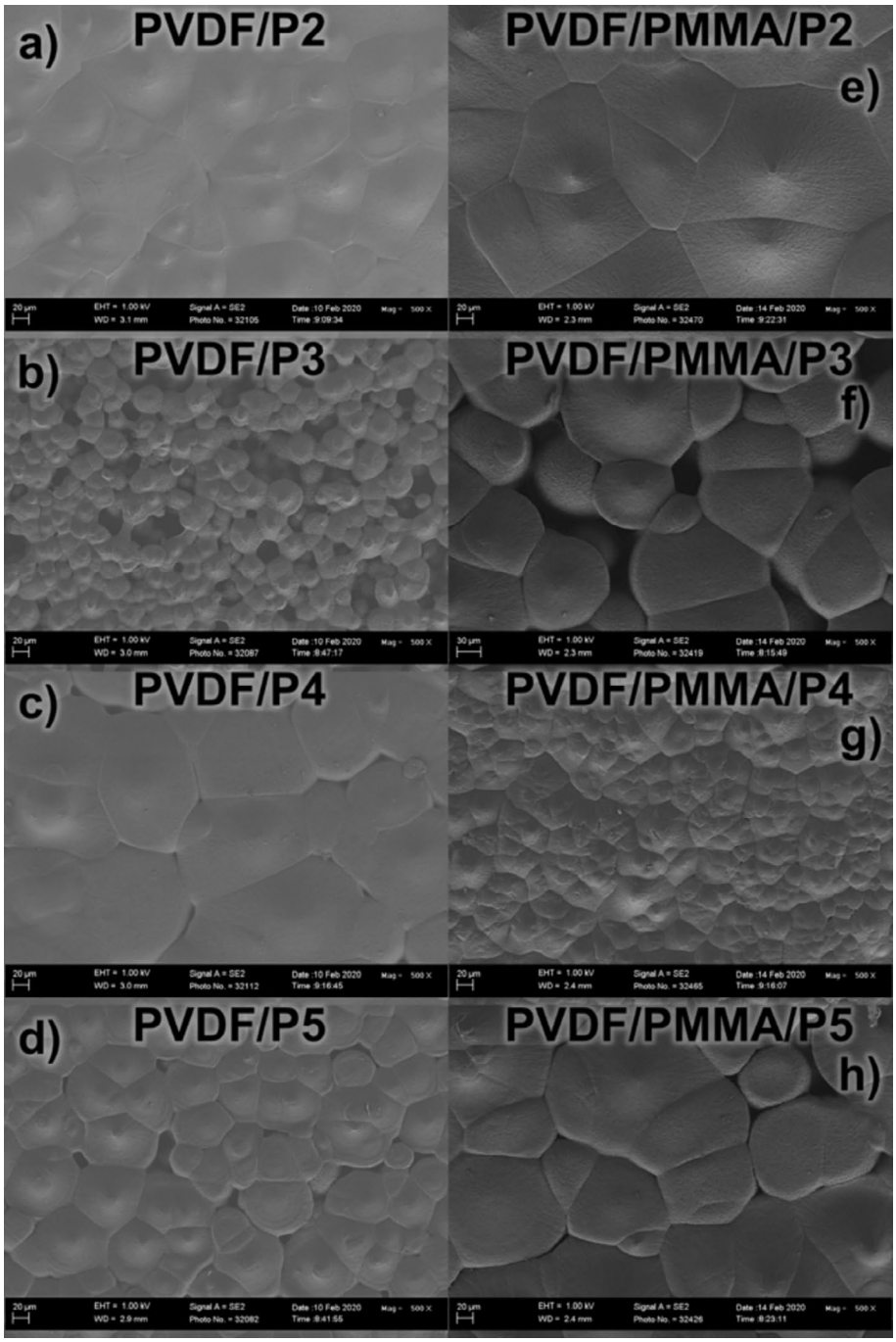

FIGURE 10 | SEM images illustrating the surface morphology comparison of plasticized PVDF reference films with PVDF-based plasticized films containing 10 wt% PMMA. The images are at 500× magnification with a 20-μm scale bar (except for (f), which has a 30 μm scale bar).

also be considered that the addition of plasticizers might be affecting the solvent evaporation rate due to interactions between them and the solvent, which might also be affecting the surface morphology observed.

As a reference for comparison, plasticized PVDF films without PMMA were produced and cast on a glass substrate using the same method described. The surface morphology of these samples is shown in Figure 10 (a–d). The difference between the plasticized PVDF films and the plasticized PVDF/PMMA films is quite stark. For samples containing P2, P3, and P5, the addition of PMMA increased spherulite size, with the most pronounced effect observed in the sample containing P3 (Figure 10 (b and f)). Polymer crystal growth is primarily influenced by two factors: the solvent evaporation rate and the nucleation rate. These factors are interrelated, but the solvent evaporation rate typically has a more dominant influence [34–38].

The interaction between the solvent and the glass substrate, as demonstrated, reduces the solvent evaporation rate. Introducing additives, such as plasticizers or PMMA, alters this dynamic. The porous surface morphology observed in the PVDF/P3 sample (Figure 10b) indicates that the addition of P3 significantly accelerated solvent evaporation. This effect surpassed the

influence of the solvent–substrate interaction, leading to rapid nucleation. The swift growth process likely entrapped solvent within the matrix, explaining the pronounced porosity in the resulting structure.

Among the plasticizers, P3 exhibited the weakest intermolecular interactions with DMAc due to its low polarity, attributed to nonpolar butyl groups that reduce dipole–dipole interactions and overall affinity for DMAc. This characteristic allows for unimpeded solvent evaporation, potentially even accelerating the process. Studies [50, 51] have shown that plasticizers can increase the solvent diffusion coefficient by raising the free volume within the system. Faster evaporation restricts the time available for crystal growth, resulting in smaller spherulites and an elevated nucleation rate. However, the addition of PMMA counteracted this by reducing the solvent evaporation rate. PMMA's strong dipole–dipole interactions with DMAc, stemming from its high polarity, prolonged the solvent retention time. This extended time allowed P3 and PMMA to enhance PVDF chain mobility, leading to the formation of fewer but larger crystals (Figure 10f). The decrease in the degree of crystallinity, from 63% in PVDF/P3 to 52% in PVDF/PMMA/P3 (Figure 9), reflects this shift in crystallization dynamics.

Plasticizer P2 exhibits stronger intermolecular forces with DMAc compared to P3, due to its ester groups, which enable more robust dipole–dipole interactions. The addition of P2 to PVDF (Figure 10a) slowed the solvent evaporation rate, leading to the formation of larger spherulites. When combined with PMMA, which also interacts strongly with DMAc, the evaporation rate was further reduced, resulting in even larger spherulite growth. This combined effect highlights the interplay between solvent dynamics and crystal growth.

The addition of PMMA caused a significant decrease in the degree of crystallinity, dropping from 67% in PVDF/P2 to 51% in PVDF/PMMA/P2 (Figure 9). The stronger combined interaction of PMMA and P2, compared to P3, likely amplified PMMA's capacity to disrupt the self- and mutual diffusion of PVDF chains. This disruption inhibited chain alignment and increased the proportion of the amorphous phase, contributing to the observed reduction in crystallinity.

The interaction between DMAc and P5 lies between that of P2 and P3 in strength. As a result, the presence of P5 increases the solvent evaporation rate, though not as significantly as P3, as evidenced by the larger spherulites observed in Figure 10d. This increased evaporation rate contributed to the porous surface morphology of the plasticized PVDF film. When PMMA was added, the spherulite size increased further, but unlike other systems, the degree of crystallinity rose from 45% in PVDF/P5 to 53% in PVDF/PMMA/P5 (Figure 9).

This result contrasts with the trends observed for other plasticizers, where PMMA typically reduces the degree of crystallinity. The unexpected increase may stem from the specific interactions between P5 and PMMA. While the addition of PMMA slows the solvent evaporation rate, as reflected in the larger spherulite size (Figure 10h), the rise in crystallinity suggests that the combination of PMMA and P5 diminishes their individual capacity to enhance the PVDF amorphous content. This interplay may favor the alignment of PVDF chains into crystalline regions, counteracting the usual trend of increased amorphous phase content. Interestingly, the melting temperature decreased by 2°C with the addition of PMMA, indicating that even though the crystallinity increased, the perfection of the crystals decreased slightly.

The surface morphology of the samples containing P4 exhibited a distinct trend compared to other systems, with a significant reduction in spherulite size following the addition of PMMA. Plasticizer P4 has the strongest interaction with DMAc, driven by its ester groups, ether linkages, and aromatic rings, which facilitate robust dipole–dipole interactions. This strong interaction is evident in Figure 10c, where the solvent evaporation rate was reduced significantly, resulting in the formation of much larger spherulites compared to other plasticized PVDF films. It seems that the interaction between DMAc and P4 exaggerated the decreased solvent evaporation rate.

When PMMA was introduced, the spherulite sizes decreased dramatically and became more evenly distributed. This change suggests that the strong polar interactions between PMMA and P4 facilitated a more uniform dispersion throughout the PVDF matrix. The morphology shown in Figure 10g indicates that P4 may enhance the nucleating effects of PMMA or that both P4 and PMMA act as nucleating agents, collectively promoting the formation of smaller crystals.

Although the strong interactions between P4, PMMA, and DMAc would typically be expected to further reduce the solvent evaporation rate, leading to larger spherulites, the observed morphology suggests that the nucleation rate played a more dominant role. This higher nucleation rate overrode the effect of slower solvent evaporation, resulting in smaller, more uniformly distributed spherulites. This is supported by the fact that the crystallization temperature of the PVDF/PMMA/P4 mixture increased from 118°C (PVDF/P4) to 121°C.

Table 3 shows that the heat of fusion of most of the plasticized PMMA-containing films decreased compared to the reference PVDF Film, PVDF/PMMA/10, and plasticized PVDF films. With all of the PMMA-plasticized films, the heat of fusion decreased in comparison to the plasticized PVDF films except for sample PVDF/PMMA/P5, which increased. This aligns with the increase in the degree of crystallinity observed.

The decrease in the heat of fusion implies that despite the significant increase in the degree of crystallinity and spherulite sizes (except for sample PVDF//PMMA/P4), the crystals formed are less stable or less perfect. A decrease in the heat of crystallization combined with an increase in the degree of crystallinity also supports this notion. Interestingly, the addition of PMMA to plasticized PVDF samples containing P3 and P5 caused a slight increase in the heat of crystallization. In the case of film PVDF/PMMA/P3, the degree of crystallinity decreases with the addition of PMMA. Hence, the increase in the heat of crystallization is an indication that the crystals formed contain fewer defects. Whereas the increase in both the heat of fusion and heat of crystallization for sample PVDF/PMMA/P5 compared to PVDF/P5 is a direct result

of the increase in the degree of crystallinity observed with the addition of PMMA to the plasticized film blend.

3.3.1.2 | DMTA Analysis. The glass transitionin temperature of the PVDF/PMMA/10 thin film was measured using DMTA analysis. The Tan δ curve for this sample is shown in Figure 11. The sample showed two discernible peaks, which indicated that the two polymers may not be completely miscible. These results show that the polymer blend exhibits phase separation into PVDF-rich and PMMA-rich domains because of limited miscibility in line with the results shown by [52]. According to their findings, solutions with low concentrations of PMMA underwent spinodal decomposition during the solvent evaporation process. However, the PVDF/PMMA/10 polymer blend showed no sign of separate peaks in the melting and crystallization DSC curves, indicating that the two polymers are compatible at these temperature ranges.

TABLE 3 | The enthalpy of fusion and crystallization for the PVDF/PMMA/plasticizer blends compared to that of the reference PVDF Film, PVDF/PMMA/10, and plasticized PVDF reference films.

Sample	ΔH_{fus} ($J\,g^{-1}$)	ΔH_C ($J\,g^{-1}$)
PVDFFilm	32.25	43.51
PVDF/PMMA/10	44.15	57.47
PVDF/P2	35.15	31.15
PVDF/P3	32.90	25.35
PVDF/P4	26.43	28.55
PVDF/P5	23.69	29.81
PVDF/PMMA/P2	26.66	29.77
PVDF/PMMA/P3	26.97	28.41
PVDF/PMMA/P4	23.08	26.43
PVDF/PMMA/P5	27.80	32.34

The formation of distinct phase separation was also found in the investigations performed by [18, 41, 53] showed that PVDF/PMMA blends higher than 90/10 showed one uniform T_g peak, whereas the investigations by [41, 53] contradicted this finding as their studies showed that blends containing PVDF compositions higher than 60 wt% had two distinct T_g peaks. These results correspond with the findings in the current investigation. Two separate T_g peaks were measured for all the PVDF/PMMA samples analyzed in this investigation (results of 30 wt% and 50 wt% PMMA not shown). As suggested by both [41, 53] the T_g peak at 71°C corresponds with the mixed amorphous phase containing both polymers, and the broad T_g curve peaking at approximately –10°C corresponds to the amorphous fraction of the pure crystalline PVDF. The big broad secondary peak is evident of the high crystallinity of the film at this concentration.

The interfaces between PVDF-rich and PMMA-rich phases may have unique compositions and interactions, contributing to the observed thermal transitions and the broadening of the observed PVDF T_g curve. Some degree of miscibility at the phase boundaries can lead to transitional regions that affect the overall thermal behavior. In comparison, the T_g DMA curve of sample PVDF/PMMA/P3 is shown in Figure 12. A distinct single, sharp T_g curve was observed for the sample with a secondary, very small peak at approximately 17°C. The thermal behavior observed across all the plasticized PVDF-based films was generally similar, with one notable exception: the absence of a secondary, smaller peak. This absence suggests that plasticizers such as P2, P4, and P5 are more effective at compatibilizing PVDF and PMMA within the amorphous phase, likely due to their stronger interaction forces with PMMA compared to P3. These findings imply that the plasticizers not only plasticize but also act as compatibilizers at the low PMMA concentrations used in this study, enhancing the

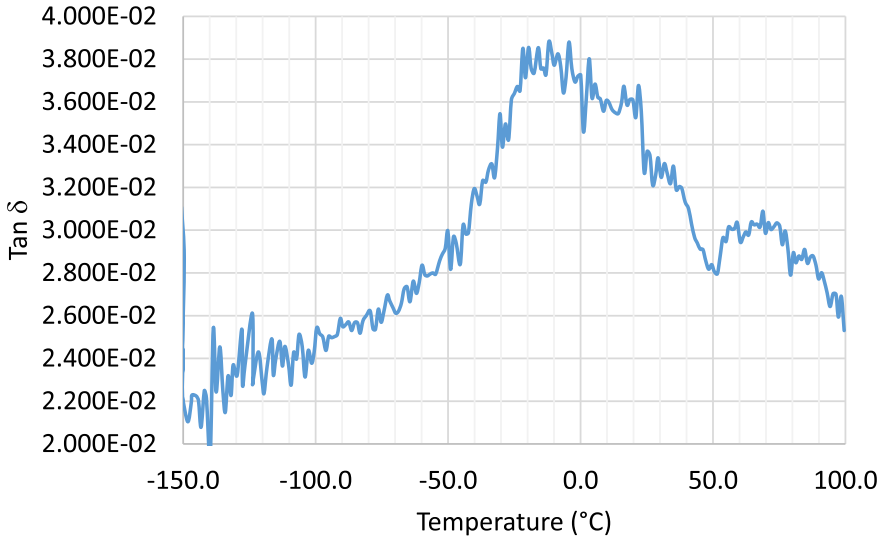

FIGURE 11 | Tan δ as a function of temperature for the PVDF/PMMA/10 sample film. The graph shows the glass transition temperature curve of the sample. [Color figure can be viewed at wileyonlinelibrary.com]

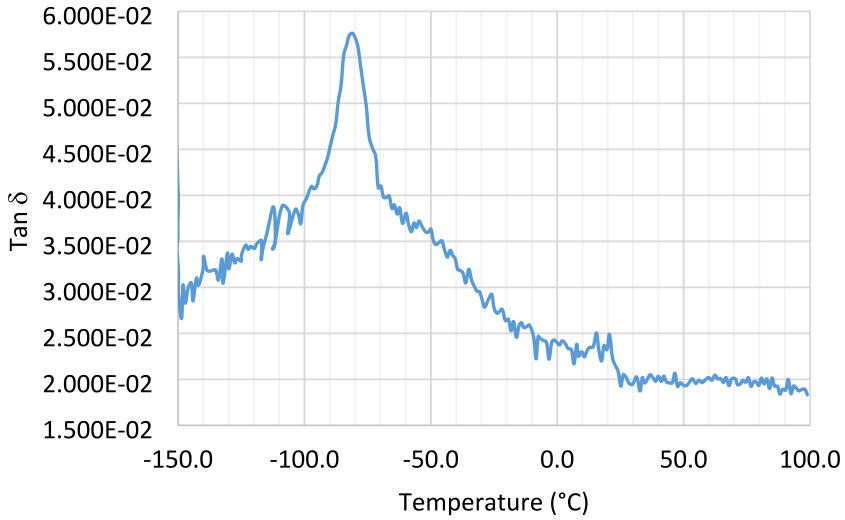

FIGURE 12 | Tan δ as a function of temperature for the PVDF/PMMA/P3 sample film. The figure shows the glass-transition temperature curve of the sample. [Color figure can be viewed at wileyonlinelibrary.com]

TABLE 4 | Glass transitioning temperature comparison of the reference PVDFFilm with different plasticized films.

Sample	T_g (°C)
PVDFFilm	−37.23
PVDF/PMMA/P2	−33.66
PVDF/PMMA/P3	−81.4
PVDF/PMMA/P4	−44.59
PVDF/PMMA/P5	−58.32

miscibility, compatibility, and homogeneity of the amorphous phases of the two polymers.

Table 4 compares the glass transition temperatures (T_g) of the various PVDF-based PMMA plasticized films examined in this study. Samples containing plasticizers P3 to P5 exhibited a large decrease in T_g, with the PVDF/PMMA/P3 blend showing the most significant reduction. This lowering of T_g suggests enhanced polymer chain mobility and increased flexibility of the films, which is advantageous for coating applications on flexible substrates like PVC architectural tarps. In contrast, the T_g of the PVDF/PMMA/P2 sample increased slightly, indicating a potential increase in rigidity. P2's propylene glycol units may not interact as effectively with PVDF due to steric hindrance. A stronger interaction with PMMA may restrict chain mobility, leading to an increase in the T_g. This increase implies that the PVDF/PMMA/P2 blend may not be suitable as a coating material for PVC tarps, where flexibility is a critical property. It also may indicate that P2 to not as effective in compatibilizing PVDF and PMMA and plasticizing the blend in general.

Although the PVDF/PMMA/P3 blend emerges as a promising candidate due to its significant T_g reduction, it is crucial to consider the surface morphology of the coating on PVC, as it profoundly affects the coating's performance and durability. As depicted in Figure 6, the surface morphology of the different PVDF/PMMA coating compositions changes markedly from the as-cast films to the dip-coated PVC tarps. These morphological transformations include variations in surface roughness, component interactions, homogeneity, and microstructural features, which can influence factors such as substrate adhesion, mechanical properties, and resistance to environmental degradation.

3.3.2 | Plasticized Coating Analysis

3.3.2.1 | SEM Analysis. The surface morphology of the plasticized PVDF/PMMA coatings produced via dip coating is shown in Figure 13. Comparing Figure 13 with the images of the same samples in Figure 10 highlights the significant impact of the casting or coating substrate on the surface morphology of the applied coating. All of the samples display a notable reduction in PVDF spherulite size compared to those observed in Figure 10 (e–h) for each of the plasticized coatings. At the same magnification used in Figure 10, the coatings in Figure 13 (a–d) appear smooth and uniform. Only at a higher magnification of 5000×, shown in Figure 13 (e–h), do the differences in surface morphologies of each plasticized coating become apparent. The altered surface morphology is primarily linked to the enhanced wettability of the PVC surface, a result of stronger interactions between the polymer and the surface. These interactions accelerate the rate of solvent evaporation, subsequently raising the nucleation rate. The inherent roughness and heterogeneity of the PVC surface further amplify this effect, facilitating the formation of smaller spherulites. Together, these factors converge to contribute to the observed changes in the surface structure.

The PVDF/PMMA/P2 coating stands out among the samples, displaying well-defined spherulites and a highly porous surface. The spherulite sizes shrink dramatically, from 60–240 μm in the glass-cast film (Figure 10e) to 2–4.5 μm in the coated sample (Figure 13e). The addition of P2 and PMMA slows the solvent evaporation rate, contributing to the formation of more distinct spherulites on the surface. The porosity likely arises from solvent entrapment, driven by a complex interaction between the polymer–substrate dynamics that increase solvent

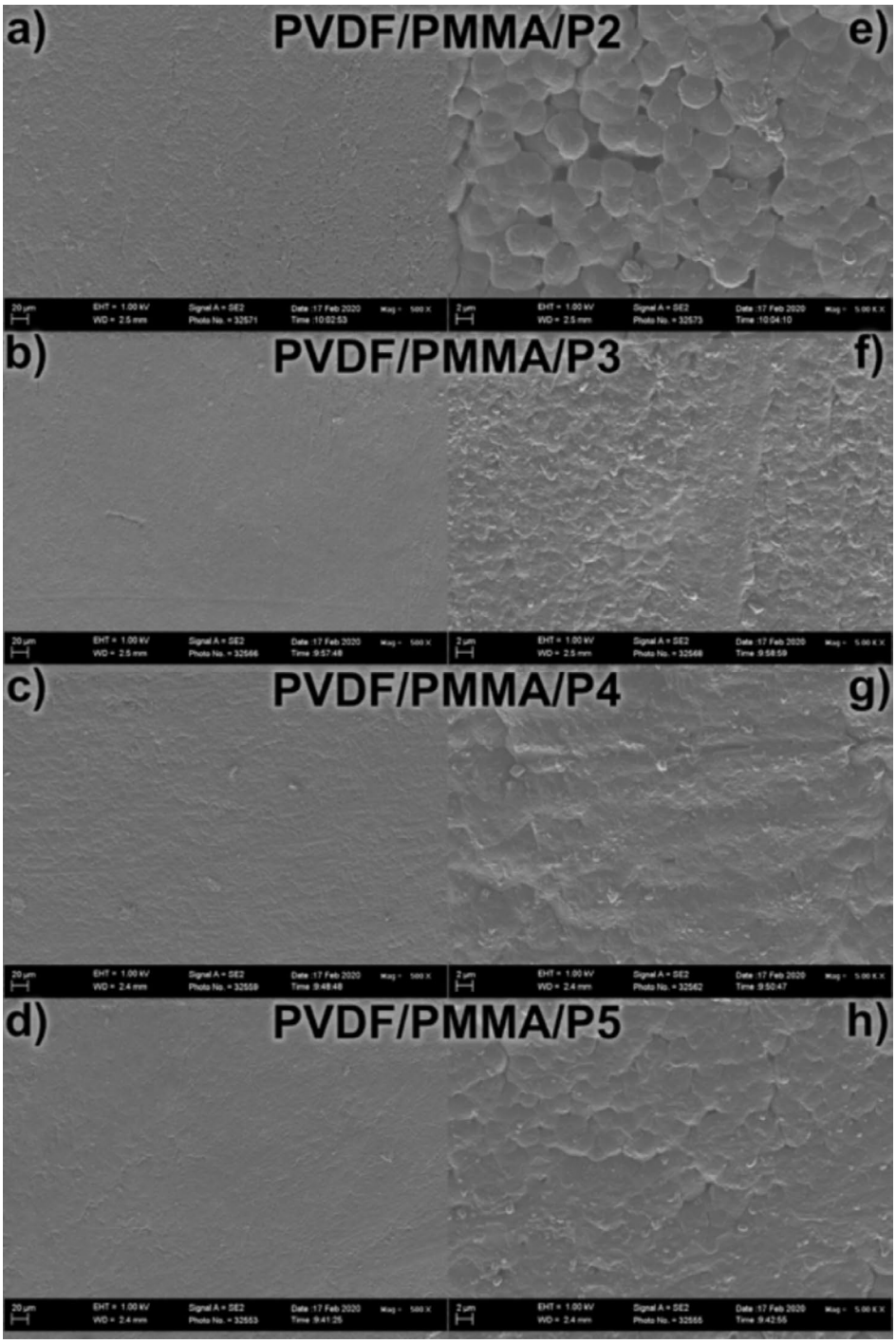

FIGURE 13 | SEM images of the surface of PVDF-based PMMA plasticized coatings dip-coated onto PVC tarp. Images (a–d) show the surface morphology at 500× magnification with a 20-μm scale bar, highlighting the overall texture of the coatings. Images (e–h) present the same surfaces at 5000× magnification with a 2-μm scale bar, revealing finer microstructural details of the coatings.

evaporation and the additives that suppress it. This variation creates a heterogeneous distribution of evaporation rates, shaping the final surface morphology. The combination of porous, uneven surface morphology and the increased rigidity identified through T_g analysis suggests that this blend is not an ideal candidate for use as a protective UV coating for architectural textiles. The structural inconsistencies and reduced flexibility would likely compromise its effectiveness and durability in such applications.

The PVDF/PMMA/P5 sample (Figure 13h) presented a mixed surface morphology, with regions of spherulite formation interspersed with smoother, amorphous areas. Spherulite size was drastically reduced by approximately 98%, from 60–200 μm in the as-cast film (Figure 10h) to 2–5 μm on the coated surface (Figure 13h), accompanied by a few observable voids. As shown by the glass-cast films, the addition of P5 increased the solvent evaporation rate slightly, while PMMA reduced it, leading to contrasting effects on the film's crystallinity in comparison to

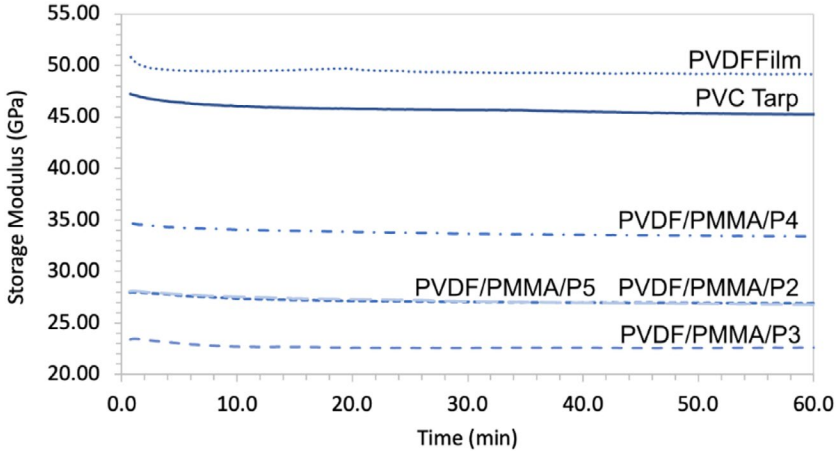

FIGURE 14 | Comparison of the storage modulus of various PVDF-based PMMA plasticized coatings on PVC tarps with that of a virgin PVC tarp and a pure PVDF-coated PVC tarp. The figure demonstrates the impact of dip-coating with different coatings on the flexibility of the PVC tarp, highlighting variations in mechanical properties introduced by each coating type. [Color figure can be viewed at wileyonlinelibrary.com]

the other plasticized films. These opposing influences, combined with the likely uneven distribution of P5 and PMMA within the PVDF matrix, resulted in a heterogeneous surface morphology featuring distinct spherulitic regions alongside amorphous structures.

Thermal analysis, including the T_g evaluation, highlighted a significant reduction in the flexibility of the blend but also highlighted the increase in the crystallinity of the blend. The increased crystallinity, coupled with the unpredictable surface morphology, raises concerns about the mechanical performance of the coated film. These characteristics make the blend unsuitable as a protective UV coating for PVC architectural textiles, where flexibility and uniformity are essential. The combination of structural inconsistencies and compromised mechanical properties diminishes its viability for such applications.

In sample PVDF/PMMA/P3 in Figure 13f, the spherulites are drastically smaller and less pronounced—barely visible—with no voids and some areas resembling the amorphous phase. The addition of P3 was shown to significantly increase the solvent evaporation rate. Even though the PMMA addition decreased the solvent evaporation rate, the plasticizer's effect, combined with the already increased evaporation rate caused by the polymer–substrate interaction, resulted in the surface morphology observed. Thermal analysis of the blend showed a significant increase in flexibility and mechanical properties due to the decreased crystallinity. All of this shows that this blend is a viable contender to be used as a protective coating.

Sample PVDF/PMMA/P4 (Figure 13g) displayed a notably smoother surface, with spherulite formation barely distinguishable, resembling an amorphous, more even surface. The addition of P4 in the glass-cast films reduced the solvent evaporation rate while amplifying PMMA's nucleation effect. This, in combination with the surface interactions, led to the formation of very small, indistinguishable spherulites, contributing to the overall smooth and amorphous-like appearance of the surface. While this blend did not reduce the film flexibility as much as the P3 blend, its superior surface characteristics and general thermal properties suggest that it may be the strongest candidate for use as a protective UV coating. More importantly, all of the plasticized coatings showed no delamination from the PVC tarp, reinforcing that the addition of 10 wt% PMMA effectively improved adhesion and the flexible coatings.

3.3.2.2 | Sample Flexibility Analysis. The flexibility of the dip-coated tarps was analyzed using an isothermal time scan in a DSC. The storage modulus of all the samples is compared in Figure 14. From the results, it is clear that all of the plasticized coating blends decreased the overall storage modulus of the dip-coated tarps. This reinforces the T_g results showing that the plasticizers do, in fact, increase the flexibility of the coatings. As a reference, a pure PVDF dip-coated sample was also analyzed. The storage modulus of this sample was higher than that of an uncoated PVC tarp, reinforcing the fact that PVDF is considered to be a rigid polymer. Interestingly, even though the T_g of sample PVDF/PMMA/P2 slightly increased, the time scan results indicate that it had the same flexibility as sample PVDF/PMMA/P5. However, the surface morphology analysis excluded these two samples as viable protective coating blends. The storage modulus results of samples PVDF/PMMA/P3 and PVDF/PMMA/P4 reinforce their viability to be considered as protective coatings.

4 | Summary and Conclusions

This study investigated PVDF/PMMA blends with various PMMA concentrations and four different plasticizers as potential protective coatings for PVC tarps. The addition of 10 wt% PMMA increased the degree of crystallinity and enhanced adhesion to the PVC substrate, while higher PMMA concentrations (30 wt% and 50 wt%) led to amorphous structures. Based on this, the decision was made to investigate the plasticization of films containing 10 wt% PMMA exclusively to balance the enhanced adhesion with the potential negative effects that the addition of acrylic might have on the mechanical and weathering properties of the PVDF-based coating. The four plasticizers investigated were di(propylene glycol) dibenzoate, dibutyl phthalate, di(ethylene glycol) dibenzoate, and benzyl butyl phthalate.

The addition of the plasticizers to a PVDF/PMMA blend notably influenced the thermal properties and surface morphology of

the coatings. This was mostly due to their effect on the solvent evaporation rate. It was also demonstrated that the coating substrate had a significant effect on the surface morphology of the plasticized PVDF/PMMA-based films. This effect was mainly due to the interplay between the solvent–substrate and polymer–substrate interactions.

The thermal and surface morphology analysis results showed that PVDF/PMMA blends with plasticizers di(ethylene glycol) dibenzoate and benzyl butyl phthalate were the top contenders to be considered as viable UV protective coatings. Both blends showed that the plasticizers significantly increased the film flexibility, based on T_g analysis, and exhibited the most favorable surface morphologies while maintaining favorable adhesion of the coating to the substrate. The surface morphology of both samples was relatively uniform, with no porosity or voids.

It is recommended that an in-depth UV stability analysis be performed on these viable blends to determine their durability and UV-protective nature.

Author Contributions

Anya Sonnendecker: conceptualization (lead), data curation (lead), formal analysis (lead), investigation (lead), methodology (lead), project administration (lead), writing – original draft (lead), writing – review and editing (lead). **Johan Labuschagne:** funding acquisition (lead), project administration (supporting), resources (lead), writing – review and editing (supporting).

Acknowledgments

The study was financially supported by funding from the Fluorochemistry Expansion Initiative (FEI) that was managed by the South African Department of Science and Technology (DST) and also from the Council for Scientific and Industrial Research (CSIR). The authors would like to thank Professor Philip Crouse who obtained the FEI funding for the project in its original form.

Data Availability Statement

The data that support the findings of this study are available from the corresponding author upon reasonable request.

References

1. R. Dallaev, T. Pisarenko, D. Sobola, F. Orudzhev, S. Ramazanov, and T. Trčka, "Brief Review of PVDF Properties and Applications Potential," *Polymers (Basel)* 14 (2022): 4793, https://doi.org/10.3390/polym14224793.

2. R. A. Iezzi, S. Gaboury, and K. Wood, "Acrylic-Fluoropolymer Mixtures and Their Use in Coatings," *Progress in Organic Coating* 40 (2000): 55–60, https://doi.org/10.1016/S0300-9440(00)00117-X.

3. X. Gu, L. Sung, D. L. Ho, et al., "Surface and Interface Properties of PVDF/ Acrylic Copolymer Blends Before and After UV Exposure," *80th Annual Meeting Technical Program of the FSCT* 252, no. 14 (2006): 5168–5181, https://doi.org/10.1016/j.apsusc.2005.07.051.

4. C. Zhang, Z. Lu, S. D. Jiang, and J. Qian, "Fabrication of Poly(Vinylidene Fluoride)-Based Composite Powder Coating With Enhanced Adhesion Performance," *Journal of Applied Polymer Science* 141, no. 6 (2024): e54918, https://doi.org/10.1002/app.54918.

5. A. Sonnendecker, D. Viljoen, B. Ameduri, and P. Crouse, "Chapter 10 - Fluoropolymer-Based Architectural Textiles: Production, Processing, and Characterization," in *Fascinating Fluoropolymers and Their Applications*, ed. B. Ameduri and S. Fomin (Elsevier, 2020), 337–399, https://doi.org/10.1016/B978-0-12-821873-0.00010-2.

6. "Lumiflon, Formulating Highly- Weatherable, Low VOC Liquid and Powder Coatings With FEVE Fluoropolymer Resin Technology." 2017.

7. B. Ameduri, "From Vinylidene Fluoride (VDF) to the Applications of VDF-Containing Polymers and Copolymers: Recent Developments and Future Trends," *Chemical Reviews* 109 (2009): 6632–6686, https://doi.org/10.1021/cr800187m.

8. D. Chun-hui, W. Li-Guang, and X. You-yi, "Crystal Behaviour and Compatibility of PVDF-Plasticizer Blend System," *Journal of Functional Polymers* 23 (2010): 155–159.

9. Z. Song, M. Xing, J. Zhang, B. Li, and S. Wang, "Determination of Phase Diagram of a Ternary PVDF/γ-BL/DOP System in TIPS Process and Its Application in Preparing Hollow Fiber Membranes for Membrane Distillation," *Separation and Purification Technology* 90 (2012): 221–230, https://doi.org/10.1016/j.seppur.2012.02.043.

10. C. H. Du, Y. Y. Xu, and B. K. Zhu, "Plasticizer Effect of Dibutyl Phthalate on the Morphology and Mechanical Properties of Hard Elastic Poly(Vinylidene Fluoride) Fibers," *Journal of Applied Polymer Science* 114 (2009): 3645–3651, https://doi.org/10.1002/app.30105.

11. B. A. Newman, J. I. Scheinbeim, and A. Sen, "The Effect of Plasticizer on the Piezoelectric Properties of Unoriented Polyvinylidene Fluoride Films," *Ferroelectrics* 57 (1984): 229–241, https://doi.org/10.1080/00150198408012765.

12. A. Marigo, C. Marega, M. Bassi, M. Fumagalli, and A. Sanguineti, "Structure and Characterization of Poly[(Vinylidene Flouride)-co-Hexafluoropropene]-(Dibutyl Phthalate) Blends," *Polymer International* 50 (2001): 449–455, https://doi.org/10.1002/pi.656.

13. A. Bré, M. Mollard, and M. Osgan, "Polyvinylidene Fluoride Compositions of Improved Flexibility and Their use, Particularly in the Manufacture of Flexible Tubes, US4584215." 1986.

14. P. Saldaña-Baqué, J. W. Strutton, R. Shankar, S. E. Morgan, and J. M. McCollum, "Exploiting Partial Solubility in Partially Fluorinated Thermoplastic Blends to Improve Adhesion During Fused Deposition Modeling," *Materials* 15 (2022): 8062, https://doi.org/10.3390/ma15228062.

15. D. Silagy, P. Bussi, and G. Marot, "Technology and Material Design in PVDF Protected Thermoplastic Substrates," *Journal of Fluorine Chemistry* 104 (2000): 79–86.

16. W. Ma, J. Zhang, and X. Wang, "Effect of Initial Polymer Concentration on the Crystallization of Poly (Vinylidene Fluoride)/poly (Methyl Methacrylate) Blend From Solution Casting," *Journal of Macromolecular Science, Part B: Physics* 47 (2008): 139–149, https://doi.org/10.1080/00222340701746127.

17. B. S. Morra and R. S. Stein, "Melting Studies of Poly(Vinylidene Fluoride) and Its Blends With Poly (Methyl Methacrylate)," *Journal of Polymer Science Polymer Physics Edition* 20 (1982): 2243–2259.

18. J. Mijović, H. Luo, and C. D. Han, "Property-Morphology Relationships of Polymethylmethacrylate/Polyvinylidenefluoride Blends," *Polymer Engineering and Science* 22 (1982): 234–240, https://doi.org/10.1002/pen.760220404.

19. I. S. Elashmawi and N. A. Hakeem, "Effect of PMMA Addition on Characterization and Morphology of PVDF," *Polymer Engineering and Science* 48 (2008): 895–901, https://doi.org/10.1002/pen.

20. E. Freire, O. Bianchi, J. N. Martins, E. E. C. Monteiro, and M. M. C. Forte, "Non-Isothermal Crystallization of PVDF/PMMA Blends Processed in Low and High Shear Mixers," *Journal of Non-Crystalline Solids* 358 (2012): 2674–2681, https://doi.org/10.1016/j.jnoncrysol.2012.06.021.

21. F. Z. Benabid, F. Zouai, A. Douibi, and D. Benachour, "Spectroscopic Study of Poly (Vinylidene Fluoride) / Poly (Methyl Methacrylate) (PVDF/PMMA) Blend," *Journal of New Technology and Materials* 5 (2015): 28–32, https://doi.org/10.12816/0019430.

22. H. Saito, T. Okada, T. Hamane, and T. Inoue, "Crystallization Kinetics in Mixtures of Poly(Vinylidene Fluoride) and Poly(Methyl Methacrylate): Two-Step Diffusion Mechanism," *Macromolecules* 24 (1991): 4446–4449, https://pubs.acs.org/sharingguidelines.

23. Z. Dou, R. Wan, H. Shen, X. Sun, H. Li, and S. Yan, "Influence of Poly(Methyl Methacrylate) on the Structure and Phase Transition Behavior of Poly(Vinylidene Fluoride)," *Polymer (Guildford)* 288 (2023): 126466, https://doi.org/10.1016/j.polymer.2023.126466.

24. A. Naruke, X. Liang, K. Nakajima, and T. Nishi, "Morphological Characterization of the Novel Fine Structure of the PMMA/PVDF Blend," *Polymer Journal* 54 (2022): 783–792, https://doi.org/10.1038/s41428-022-00625-z.

25. S. M. Pawde and K. Deshmukh, "Investigation of the Structural, Thermal, Mechanical, and Optical Properties of Poly(Methyl Methacrylate) and Poly(Vinylidene Fluoride) Blends," *Journal of Applied Polymer Science* 114 (2009): 2169–2179, https://doi.org/10.1002/app.30641.

26. T. Nishiyama, T. Sumihara, E. Sato, and H. Horibe, "Effect of Solvents on the Crystal Formation of Poly (Vinylidene Fluoride) Film Prepared by a Spin-Coating Process," *Polymer Journal* 49 (2017): 319–325, https://doi.org/10.1038/pj.2016.116.

27. P. H. C. Eilers, "A Perfect Smoother," *Analytical Chemistry* 75 (2003): 3631–3636, https://doi.org/10.1021/ac034173t.

28. M. Gu, J. Zhang, X. Wang, and W. Ma, "Crystallization Behavior of PVDF in PVDF-DMP System via Thermally Induced Phase Separation," *Journal of Applied Polymer Science* 102 (2006): 3714–3719, https://doi.org/10.1002/app.24531.

29. J. Sun, L. Yao, Q. L. Zhao, et al., "Modification on Crystallization of Poly(Vinylidene Fluoride) (PVDF) by Solvent Extraction of Poly(Methyl Methacrylate) (PMMA) in PVDF/PMMA Blends," *Frontiers of Materials Science* 5 (2011): 388–400, https://doi.org/10.1007/s11706-011-0152-2.

30. X. Zhao, J. Cheng, J. Zhang, S. Chen, and X. Wang, "Crystallization Behavior of PVDF/PMMA Blends Prepared by In Situ Polymerization From DMF and Ethanol," *Journal of Materials Science* 47 (2012): 3720–3728, https://doi.org/10.1007/s10853-011-6221-1.

31. K. Nakagawa and Y. Ishida, "Annealing Effects in Poly(Vinylidene Fluoride) as Revealed by Specific Volume Measurements, Differential Scanning Calorimetry, and Electron Microscopy," *Journal of Polymer Science Part B: Polymer Physics* 11 (1973): 2153–2171, https://doi.org/10.1002/pol.1973.180111107.

32. I. Y. Abdullah, M. Yahaya, M. H. H. Jumali, and H. M. Shanshool, "Influence of the Substrate on the Crystalline Phase and Morphology of Poly (Vinylidene Fluoride) (PVDF) Thin Film," *Surface Review and Letters* 23 (2016): 1650005, https://doi.org/10.1142/S0218625X16500050.

33. D. F. S. Petri, "Characterization of Spin-Coated Polymer Films," *Journal of the Brazillian Chemical Society* 13, no. 5 (2002): 695–699, https://doi.org/10.1590/S0103-50532002000500027.

34. K. Pramod and R. B. Gangineni, "Influence of Solvent Evaporation Rate on Crystallization of Poly(Vinylidene Fluoride) Thin Films," *Bulletin of Materials Science* 38 (2015): 1093–1098, https://doi.org/10.1007/s12034-015-0894-z.

35. Y. Zhao, Y. Zhou, Y. Yang, J. Xu, Z. D. Chen, and Y. Jiang, "The Impact of Solvents on Properties of Solution-Cast Poly(Vinylidene Fluoride) Films for Energy Storage," *Materials Letters* 219 (2018): 201–204, https://doi.org/10.1016/j.matlet.2018.02.110.

36. K. E. Strawhecker, S. K. Kumar, J. F. Douglas, and A. Karim, "The Critical Role of Solvent Evaporation on the Roughness of Spin-Cast Polymer Films," *Macromolecules* 34 (2001): 4669–4672, https://doi.org/10.1021/ma001440d.

37. Í. López García, J. L. Keddie, and M. Sferrazza, "Probing the Early Stages of Solvent Evaporation and Relaxation in Solvent-Cast Polymer Thin Films by Spectroscopic Ellipsometry," *Surface and Interface Analysis* 43 (2011): 1448–1452, https://doi.org/10.1002/sia.3728.

38. C. Schaefer, P. Van Der Schoot, and J. J. Michels, "Structuring of Polymer Solutions Upon Solvent Evaporation," *Physical Review. E, Statistical, Nonlinear, and Soft Matter Physics* 91 (2015): 022602, https://doi.org/10.1103/PhysRevE.91.022602.

39. R. Gregorio, Jr. and N. C. P. d. S. Nociti, "Effect of PMMA Addition on the Solution Crystallization of the Alpha and Beta Phases of Poly(Vinylidene Fluoride) (PVDF)," *Journal of Physics D: Applied Physics R* 28 (1995): 432–436.

40. D. R. Paul, J. W. Barlow, R. E. Bernstein, and D. C. Wahrmund, "Polymer Blends Containing Poly(Vinylidene Fluoride). Part IV: Thermodynamic Interpretations," *Polymer Engineering and Science* 18, no. 16 (1978): 1225–1234, https://doi.org/10.1002/pen.760181607.

41. B. Lu, K. Lamnawar, A. Maazouz, and H. Zhang, "Revealing the Dynamic Heterogeneity of PMMA/PVDF Blends: From Microscopic Dynamics to Macroscopic Properties," *Soft Matter* 12 (2016): 3252–3264, https://doi.org/10.1039/c5sm02659h.

42. S. J. Ebbens and J. P. S. Badyal, "Surface Enrichment of Fluorochemical-Doped Polypropylene Films," *Langmuir* 17 (2001): 4050–4055, https://doi.org/10.1021/la010081s.

43. N. Belhaneche-Bensemra, B. Belaabed, and A. Bedda, "Study of the Miscibility and the Thermal Degradation of PVC/PMMA Blends," in *Macromol Symp* (John Wiley and Sons Ltd, 2002), 203–216, https://doi.org/10.1002/1521-3900(200203)180:1<203::AID-MASY203>3.0.CO;2-H.

44. M. Dixit, V. Mathur, M. Baboo, et al., "Investigation of Miscibility and Mechanical Properties of PMMA/PVC Blends," *Optoelectronics and Advanced Materials, Rapid Communications* 3 (2009): 1099, https://www.researchgate.net/publication/286968639–1105.

45. M. S. Khan, R. A. Qazi, and M. S. Wahid, "Miscibility Studies of PVC/PMMA and PS/PMMA blends by dilute solution viscometry and FTIR." 2008, http://www.academicjournals.org/AJPAC.

46. E. Fekete, E. Földes, and B. Pukánszky, "Effect of Molecular Interactions on the Miscibility and Structure of Polymer Blends," *European Polymer Journal* 41 (2005): 727–736, https://doi.org/10.1016/j.eurpolymj.2004.10.038.

47. K. Aouachria and N. Belhaneche-Bensemra, "Miscibility of PVC/PMMA Blends by Vicat Softening Temperature, Viscometry, DSC and FTIR Analysis," *Polymer Testing* 25 (2006): 1101–1108, https://doi.org/10.1016/j.polymertesting.2006.07.007.

48. A. A. Yousefi, "Influence of Polymer Blending on Crystalline Structure of Polyvinylidene Fluoride," *Iranian Polymer Journal* 20 (2011): 109–121.

49. A. Marcilla and M. Beltrán, "Mechanisms of Plasticizers Action," in *Handbook of Plasticizers*, 3rd ed., ed. G. Wypych (ChemTec Publishers, 2017), 119–134.

50. M. Rawat and S. Ahuja, "Residual Solvent Minimization in Polystyrene-p-Xylene Coatings Using a Nonvolatile Additive," *Journal of Applied Polymer Science* 138 (2021): 50399, https://doi.org/10.1002/app.50399.

51. G. S. Park and M. Saleem, "Diffusion of Additives and Plasticisers in poly(vinyl chloride) - V. Diffusion of n-Hexadecane and DDT in Various Poly(vinyl chloride)/Dialkylphthalate Compositions." 1984.

52. C. Huang and L. Zhang, "Miscibility of Poly(Vinylidene Fluoride) and Atactic Poly(Methyl Methacrylate)," *Journal of Applied Polymer Science* 92 (2004): 1–5, https://doi.org/10.1002/app.13564.

53. S. Wu, "Entanglement Between Dissimilar Chains in Compatible Polymer Blends: Poly(Methyl Methacrylate) and Poly(Vinylidene Fluoride)," *Journal of Polymer Science Part B: Polymer Physics* 25 (1987): 557–566, https://doi.org/10.1002/polb.1987.090250308.